

Calibration of RPC-based muon detector at BESIII^{*}

XIE Yu-Guang(谢宇广)^{1,2;1)} LI Wei-Dong(李卫东)¹ LIANG Yu-Tie(梁羽铁)³ YOU Zheng-Yun(尤郑昀)³
 MAO Ya-Jun(冒亚军)³ ZHANG Jia-Wen(张家文)¹ BIAN Jian-Ming(边渐鸣)^{1,2} CAO Guo-Fu(曹国富)^{1,2}
 CAO Xue-Xiang(曹学香)^{1,2} CHEN Shen-Jian(陈申见)⁴ DENG Zi-Yan(邓子艳)¹
 FU Cheng-Dong(傅成栋)^{1,5} GAO Yuan-Ning(高原宁)⁵ HE Kang-Lin(何康林)¹ HE Miao(何苗)^{1,2}
 HUA Chun-Fei(花春飞)⁶ HUANG Bin(黄彬)^{1,2} HUANG Xing-Tao(黄性涛)⁷ JI Xiao-Bin(季晓斌)¹
 LI Fei(李飞)¹ LI Hai-Bo(李海波)¹ LIU Chun-Xiu(刘春秀)¹ LIU Hua-Min(刘怀民)¹
 LIU Qiu-Guang(刘秋光)^{1,2} LIU Suo(刘锁)⁸ LIU Ying-Jie(刘英杰)¹ MA Qiu-Mei(马秋梅)¹
 MA Xiang(马想)^{1,2} MAO Ze-Pu(毛泽普)¹ MO Xiao-Hu(莫晓虎)¹ PAN Ming-Hua(潘明华)⁹
 PANG Cai-Ying(庞彩莹)⁹ PING Rong-Gang(平荣刚)¹ QIN Ya-Hong(秦亚红)⁶ QIU Jin-Fa(邱进发)¹
 SUN Sheng-Sen(孙胜森)¹ SUN Yong-Zhao(孙永昭)^{1,2} WANG Ji-Ke(王纪科)^{1,2}
 WANG Liang-Liang(王亮亮)^{1,2} WEN Shuo-Pin(文硕频)¹ WU Ling-Hui(伍灵慧)^{1,2} XU Min(徐敏)¹⁰
 YAN Liang(严亮)^{1,2} YUAN Chang-Zheng(苑长征)¹ YUAN Ye(袁野)¹ ZHANG Bing-Yun(张炳云)¹
 ZHANG Chang-Chun(张长春)¹ ZHANG Jian-Yong(张建勇)¹ ZHANG Xue-Yao(张学尧)⁷
 ZHANG Yao(张瑶)¹ ZHENG Yang-Heng(郑阳恒)² ZHU Ke-Jun(朱科军)¹
 ZHU Yong-Sheng(朱永生)¹ ZHU Zhi-Li(朱志丽)⁹ ZOU Jia-Heng(邹佳恒)⁷

¹ Institute of High Energy Physics, CAS, Beijing 100049, China

² Graduate University of Chinese Academy of Sciences, Beijing 100049, China

³ Peking University, Beijing 100871, China

⁴ Nanjing University, Nanjing 210093, China

⁵ Tsinghua University, Beijing 100084, China

⁶ Zhengzhou University, Zhengzhou 450001, China

⁷ Shandong University, Jinan 250100, China

⁸ Liaoning University, Shenyang 110036, China

⁹ Guangxi Normal University, Guilin 541004, China

¹⁰ Department of Modern Physics, University of Science and Technology of China, Hefei 230026, China

Abstract The calibration algorithm for RPC-based muon detector at BESIII has been developed. The calibration method, calibration error and algorithm performance are studied. The primary results of efficiency and noise at layer, module and strip levels have been calibrated with cosmic ray data. The calibration constants are available for simulation and reconstruction tuning. The results of Monte Carlo and data are also compared to check the validation and reliability of the algorithm.

Key words calibration, RPC, BESIII, muon detector, efficiency, noise

PACS 07.05.Kf, 29.40.Gx, 87.10.Rt

1 Introduction

BESIII, a new spectrometer for the challenging physics in the tau-charm energy region, has been con-

structed and gone into the commissioning phase at BEPCII [1], the upgraded e^+e^- collider with peak luminosity up to $10^{33} \text{ cm}^{-2}\text{s}^{-1}$ in Beijing. The Resistive Plate Chambers (RPCs) have been used in the BESIII

Received 8 April 2009, Revised 5 May 2009

^{*} Supported by CAS Knowledge Innovation Project(U-602, U-34), National Natural Science Foundation of China (10491300, 10491303, 10605030, 10835001, 10821063), 100 Talents Program of CAS (U-25 and U-54) and National Basic Research Program of China (2009CB825208)

1) E-mail: ygxie@ihep.ac.cn

©2009 Chinese Physical Society and the Institute of High Energy Physics of the Chinese Academy of Sciences and the Institute of Modern Physics of the Chinese Academy of Sciences and IOP Publishing Ltd

muon counter (MUC). These RPCs are made of a new type of bakelite material with melamine treatment instead of linseed oil treatment [2]. The BESIII muon counter will mainly contribute to the distinguishing muons from hadrons, especially the pions. It is designed to be with efficiency up to 95%, spacial resolution better than 20 mm and run in the streamer mode with gas mixture of argon:F134a:iso-butane = 50:42:8.

The most notable character of RPC running in streamer mode is the big signal (normally ≥ 100 mV). Thus the efficiency, noise (e.g., noise ratio, counting rate, dark current) and spacial resolution are the main performances concerned. It's well known that the resistivity of the bakelite electrodes plays an important role in the RPC performance. Unfortunately, the resistivity is very sensitive to the environment factors, such as the temperature and humidity, so is the RPC performance [3]. RPC performance also has direct relations with the operation parameters, e.g., high voltage, threshold, gas mixture, radiation background, and so on. Furthermore, the production techniques also can not ensure that every chamber has the same performance and long-term stability. In brief, the RPC performance will vary from chamber to chamber and from time to time, that is just the necessity of calibration, especially for the efficiency and noise.

2 Calibration algorithm

2.1 Calibration parameters

So far, the quantitative relationships between the performances of RPC running in streamer mode and

their influence factors are not very clear and still under study. However, the real efficiency and noise can still be analyzed and calibrated at different levels according to the MUC detector structure.

As listed in Table 1, the efficiency, counting rate and noise ratio of each strip can be calibrated at Level 2, which is considered to be fine enough for the simulation and reconstruction. It is also helpful to calculate the efficiency and noise at the highest pad level, which can offer two dimension (2D) performance maps. In our case, however, a pad is an area of strip width square in one strip divided by reconstruction, but not a real detection unit with independent readout channel (named "pad readout") that can be built in simulation. So the results at the pad level are only used for performance monitoring and problem locating.

Table 1. Calibration parameters at different levels

level&unit	eff (%)	cnt/nosratio /(Hz/cm ²)	number
0 layer	0 ~ 100	0 ~ 2/1	9
1 module	0 ~ 100	0 ~ 2/1	136
2 strip	0 ~ 100	0 ~ 2/1	9152
3 pad	0 ~ 100	0 ~ 2/1	559910

2.2 Calibration method

The calibration is based on the matching of hits and tracks in a given window. Fig. 1 shows the details. For each track passing the selection, a loop is started to search the effective hit, fail hit and noise hit at each expected position of this track one by one. A crucial parameter in this process is the efficiency window (i.e., ω), which significantly influences the

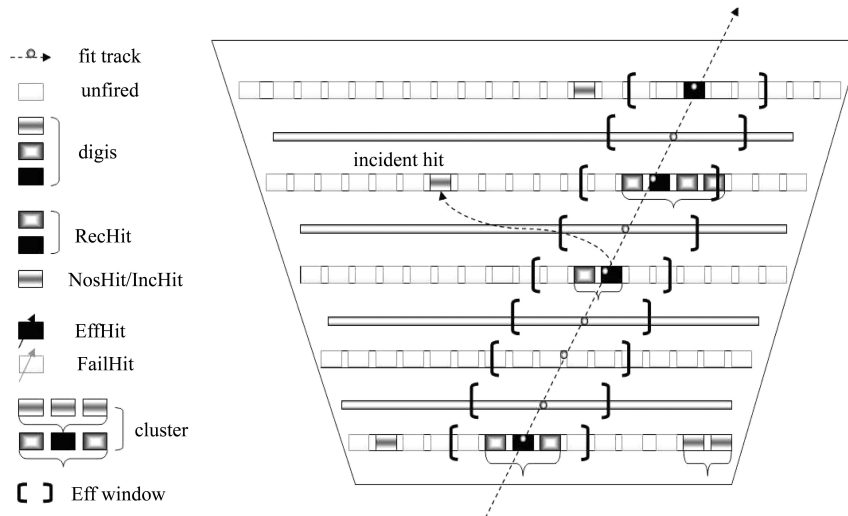


Fig. 1. The definitions of calibration parameters.

calibration result and should be chosen reasonably according to the cluster size distribution and reconstruction quality. Suppose n is the id of the strip closest to the expected position, the matching range will be $n \pm \omega$. The searching result includes three cases: 1). No strip is fired within the window, then strip n is regarded as detection failure. 2). Strip n or $n \pm i (i \leq \omega)$ is fired, then strip n or $n \pm i$ is regarded as detection success. 3). At the same segment and layer with strip n , the strip k is fired and $|k - n| > \omega$, then the strip k is deemed to be with a noise hit, no matter whether it is a real noise hit or an incident hit of this track.

Then the efficiency and noise ratio can be calculated by Eq. (1).

$$\varepsilon_{li} = \frac{m_{li}}{n_{li}}, \quad r_{li} = \frac{p_{li}}{q_{li}}, \quad (l=0,1,2), \quad (1)$$

where, ε_{li} and r_{li} are the efficiency and noise ratio of unit i at Level l , m_{li} and n_{li} indicate the number of effective hits and tracks in this unit respectively, p_{li} and q_{li} indicate the number of noise hits and fired digis respectively. In fact, if the calibration level is set as 2, then ε_{Li} and $r_{Li} (L < 2)$ can be also calculated by Eq. (2), i.e., the average value of all strips belonging to unit i at level L .

$$\varepsilon_{Li} = \frac{1}{S_{Li}} \sum_{j=0}^{S_{Li}} \varepsilon_{2j}, \quad r_{Li} = \frac{1}{S_{Li}} \sum_{j=0}^{S_{Li}} r_{2j}, \quad (L=0,1), \quad (2)$$

where, S_{Li} is the number of strips belonging to unit i at Level L . This will cause a little difference from Formula 1, but more accurate. If the statistics is enough, they are almost the same.

As for the counting rate, it can be analyzed by the random trigger data. Suppose the trigger rate is $f_{\text{trdn}} (\text{Hz})$ with time window $T_{\text{trg}} (\text{ns})$, and n_e events are acquired, then the counting rate can be calculated by:

$$c_{li} = \frac{d_{li}}{n_e T_{\text{trg}} A_{li}} \times 10^9 \text{ Hz/cm}^2, \quad (l=0,1,2), \quad (3)$$

where, d_{li} and A_{li} are the number of digis and area (cm^2) of the unit i at Level l , respectively.

Except the general way to simulate the noise by mixing noise data, the noise ratio and counting rate are the new approaches and more suitable for the RPC-based muon detector. In addition, the dark current and spacial resolution are also important, but both can not be used in the simulation, so they will not be considered in the calibration. For the former, it is monitored and recorded by the slow control system, and for the latter, it is the sigma of track residual distribution, which should be gaussian and vary with layer.

By applying the 3σ cut method to the residual distribution layer by layer, the efficiency at layer level can also be calculated. In this way, the distribution is fitted by gaussian, and the unfired residual (set as a big number) at a layer must contribute to the distribution of this layer. In fact, if the efficiency window is chosen as a reasonable value, the results by both ways should be very similar. Currently, the difference is $< 3\%$ and will be improved.

2.3 Data flow

The calibration algorithm, named MucCalibAlg, is developed with C++ in the BESIII Offline Software System (BOSS) [4], which is based on the Gaudi framework and Geant4 simulation toolkit. The data flow is illustrated in Fig. 2. The precondition of calibration is the reconstruction, which is done by the MucRecAlg algorithm [5]. The MucRecAlg offers the expected tracks collection, attached hits collection and can be run in different modes, such as extrapolation, self-reconstruction, and combined modes.

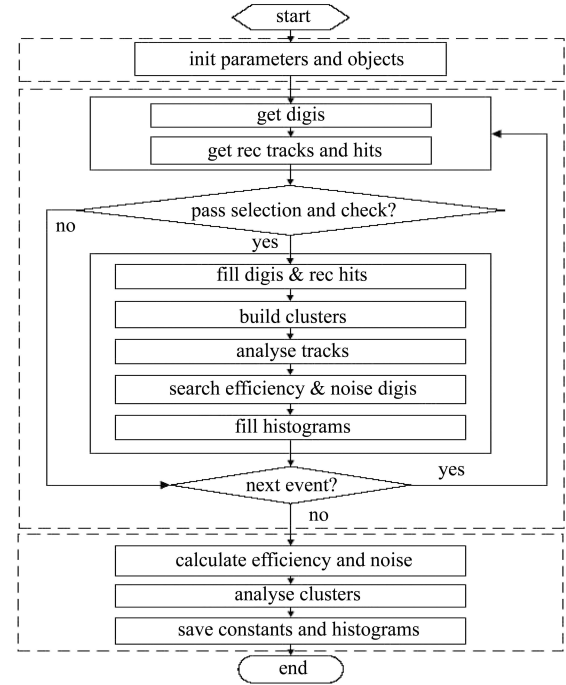


Fig. 2. The data flow of calibration algorithm.

For each event, firstly, the collections of digis (hits), expected tracks and attached hits will be retrieved from the Transient Data Store(TDS), then the event need to pass the selection and check, which can be configured according to the data types and physics requirements. The key processes in the calibration include clusters building, tracks analyzing and effective and noise hits searching. All parameters will

be calculated or fitted in the finalized module and saved to constant file in ROOT format. The calibration constant files will be organized and managed by the BESIII calibration database. The MUC simulation and reconstruction algorithms access the calibration constants via MucCalibConstSvc. The MucCalibConstSvc gets the constants from BESIII calibration service, which has the direct interface with the calibration constant database.

3 Algorithm study

3.1 Calibration error

According to the calibration method described above, the effective and noise hits obey the binomial distribution, which gives the error as:

$$\sigma_{p_{li}} = \sqrt{\frac{p_{li}(1-p_{li})}{n_{li}}}, \quad (p = \varepsilon, r; \quad l = 0, 1, 2), \quad (4)$$

where n_{li} is the number of tracks or hits. Eq. (4) implies that the error reaches the maximum when $p_{li} = 0.5$. For RPCs with 90% efficiency (conservative estimate), the number of good tracks must be greater than 800 if the error is needed to be less than 0.01, as shown in Fig. 3. This requires about 0.63 M

$$\left(N_{\mu\mu} = \frac{800}{2} \times \frac{1280(\text{MaxStrip_In_}4\pi)}{0.9(4\pi) \times 0.9(\text{eff})} \right)$$

good dimu events to ensure the precision. While corresponding to Eq. (2), the error of level 0 and 1 also can be calculated by :

$$\sigma_{p_{Li}} = \sqrt{\sum_{j=0, j < S_{Li}} \sigma_{p_{2j}}^2}, \quad (p = \varepsilon, r; L = 0, 1), \quad (5)$$

where, S_{Li} is the number of strips belonging to unit i at Level L .

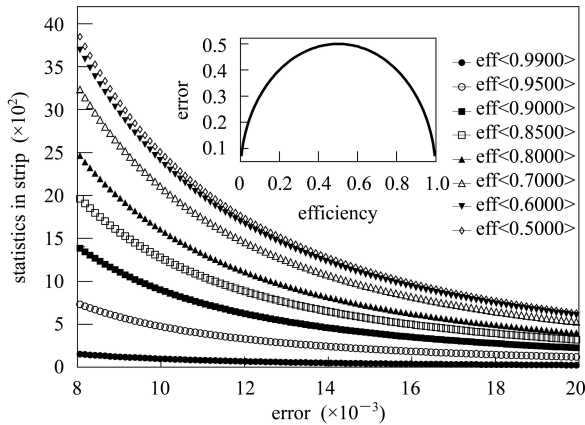


Fig. 3. The statistical error of calibration. Each curve indicates the dependency of error on statistics for a given efficiency.

The other part is the system error, which comes from the reconstruction method and the efficiency window. Table 2 lists three reconstruction modes, and the main differences are the reconstruction seed and the track extrapolation. The extrapolation precision directly affects the calibration results. The fitting method is another factor which may also be a source of system error, if the bending of tracks in MUC by magnetic field can not be ignored. But recently, the bending effect in MUC is too small to be considered.

Table 2. Three reconstruction methods.

mode	detail
0	MDC seed only, extrapolation, line/quadratic fit
1	MUC seed only, self tracking, line/quadratic fit
2	if no MDC seed, MUC seed used, line/quadratic fit

As shown in Fig. 4(a) and (b), the efficiency by Mode 0 is about 3% lower than that by Mode 1 because of the limitation of extrapolation precision (in Boss6.4.0 and lower). After improving both reconstruction modes in Boss6.4.1, this system error has been reduced to 0.5%. Fig. 4(c) and (d) show the efficiency window effect, and $\omega = 4$ is chosen, with which, the efficiency is very close to that during the RPC quality control (QC) and very similar to the results by 3σ cut method. If the window is set too wide, fake efficiency will be introduced, contrarily, the real efficiency will be lost. That the window changes one strip width may result in efficiency with $\pm 1\%$ – 8% variation (at strip level).

3.2 Calibration biases

In order to obtain reliable calibration results, the biases hiding in the reconstruction and calibration must be found out and corrected. Firstly, the outermost expected position of a track is determined by the outermost layer with hits within the reconstruction window, as shown in the boxes of Fig. 5. So the efficiency is on the higher side for these layers. The better way is to extrapolate a track to the outermost layer no matter whether there are hits or not. At the same time, we use high momentum (> 1.2 GeV/c) muon tracks, such as, dimu tracks, to do the calibration, then this bias can be avoided. Secondly, it is presumed that all physics tracks fly from inner to outer layers, so the innermost layer always has an expected position. However, because of the structure limitation, the width of layer 0 in the barrel is 15% shorter than it should be along with the “V” angle, as shown in the circles of Fig. 5. The reason is

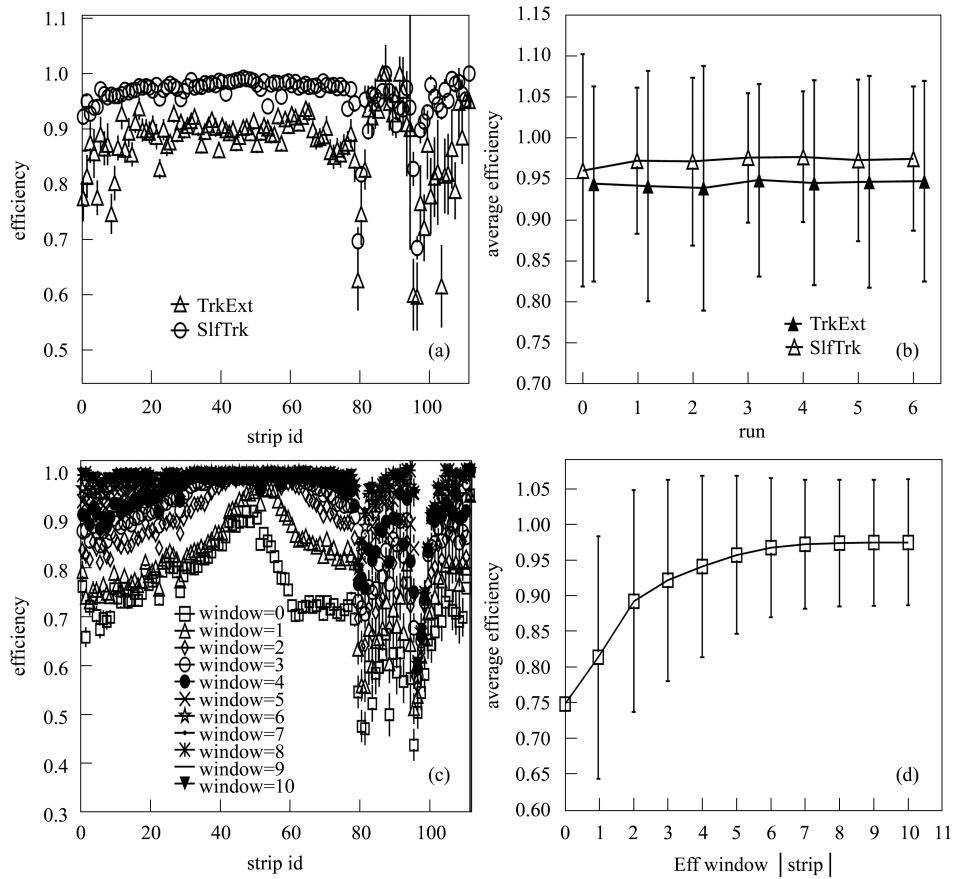


Fig. 4. The sources of system error. (a) The strip efficiency in a module by extrapolation and self reconstruction. (b) The average efficiency of strips in barrel versus run. (c) The efficiency window effect in a module. (d) The average efficiency versus window.

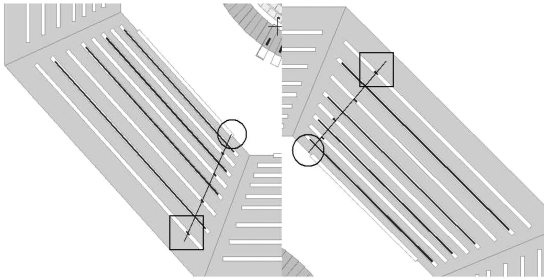


Fig. 5. The biases in MUC reconstruction and calibration.

the additional support structures on both sides of layer 0 in each segment. This will result in the efficiency on the lower side, since the reconstruction window is normally larger than 5-strip width. If the matching is constrained strictly adequate on both sides of Layer 0 in all barrel segments, the bias can be avoided. Thirdly, if a fired layer contributes to the fitting of expected track, it will result in efficiency bias (higher) in this layer. For dimu events, it is 1%–2% higher. For all events, it is even about 10% higher. The lower the momentum, the bigger the bias (because of less hits for fitting). More serious bias happens in the

self reconstruction. If some layers are chosen as seeds always, then their efficiencies are always higher than the real values. So the seed layers must be chosen at random in self reconstruction. All the above biases have been corrected in Boss6.4.1.

3.3 Algorithm performance

It's no doubt that the validation and reliability is the most important performance of an algorithm. In order to check this, here the $\Delta\varepsilon$ is used and defined as:

$$\Delta\varepsilon = \varepsilon_{\text{cal}} - \varepsilon_{\text{set}}, \quad (6)$$

where, ε_{cal} is the efficiency by calibration, and ε_{set} is the efficiency set via calibration constant service. So the $\Delta\varepsilon$ should tend to zero along with the event number increase. Fig. 6 shows the $\Delta\varepsilon$ results by the Monte Carlo $J/\psi \rightarrow \mu^+\mu^-$ events, which are produced by KKMC generator [6] in Boss6.3.5. Currently, the best results of $\Delta\varepsilon$ are -0.0128 ± 0.0204 , -0.0007 ± 0.0278 , -0.0153 ± 0.0244 at layer, module and strip level respectively. The ideal result should be 0 ± 0.01 for all levels and depends on more detailed tuning rather than increasing events.

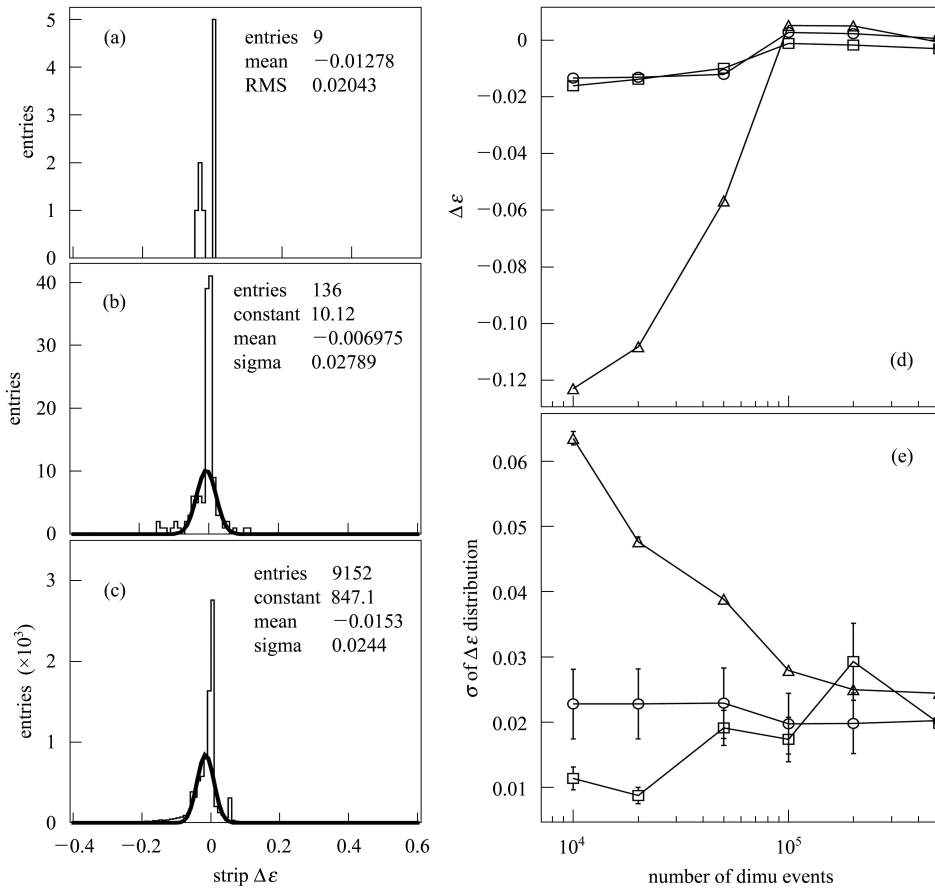


Fig. 6. The algorithm performance. (a), (b) and (c) indicate the efficiency difference distribution with 500k dimu events for layer, module and strip levels respectively. (d) shows the change tendency of $\Delta\epsilon$ of a unit (as an example) at each level and (e) illuminates the global effect at each level: layer (open circle), module (open square) and strip (open triangle up).

From a programming point of view, the processing speed and memory assumption must be considered. The test results by using real data are listed in Table 3. The speed of self reconstruction+calibration (SlfTrk, (5 ± 0.5) ms/event) is about 4–5 times faster than that of extrapolating reconstruction+calibration (TrkExt, (20 ± 3) ms/event), no matter for the single bunch or multi bunch data. As for the memory assumption, the initial memory for calibration job is about 220 MB. By using the dimu data, which have been selected and reconstructed, we can see that the speed of MucCalibAlg itself is 2.52 ms/event, and there is no memory leak.

Table 3. The test results of calibration speed.

data	recmode	job time (100k events)	speed/ (ms/event)
S-bunch	TrkExt	28:24.80	17.05
	SlfTrk	09:02.99	5.43
M-bunch	TrkExt	35:09.31	21.09
	SlfTrk	08:09.63	4.89
Dimu	–	04:12.48	2.52

4 RPC performance

By using the cosmic ray data accumulated from May to July in 2008, the muon detector had been studied and adjusted in detail. Most of the RPC performances can be obtained by MucCalibAlg, including efficiency, single counting rate, noise ratio and

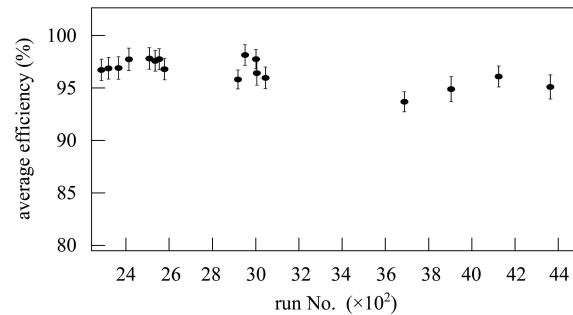


Fig. 7. The run-by-run efficiency of all RPC modules. Before Run 3400, the high voltage and discrimination threshold were 8 kV and 100 mV. After that, they were set as 7.2 ± 0.2 kV and 75 mV respectively.

spacial resolution. Fig. 7 shows the run-by-run efficiency of all RPC modules during the cosmic ray commissioning. The runs included all were taken in different days. Obviously, the efficiency is $(94\pm 1)\%$, which is very close to the design value, even though there is about 2% lower after high voltage and threshold adjustment. More detailed results can be found in Ref. [7].

5 Monte Carlo study

Monte Carlo (MC) study is an important way to debug and tune both the hardware and software. Currently, for muon detector, the real geometry with hardware alignment and detection efficiency by cosmic ray data have been applied to the MUC simulation and reconstruction. This study is done in Boss6.4.3. In order to make MC and data consistent, it is necessary to use the “natural” cosmic ray generator in the simulation. In the “natural” generator, there is only one big sampling plane on the top of the BESIII geometry to constrain the cosmic ray tracks. All MC events also must pass the same trig-

ger conditions used in the data taking. 4×10^5 real events are used for calibration and comparison from Run3006 (at random), of which the trigger condition is that the number of hits in the barrel Time-Of-Flight (TOF) is greater than one, named NBTOF2. 2M MC events are produced with 48.7% trigger efficiency of NBTOF2. The efficiency at strip level of Run3006 is the only input in the simulation. The reconstruction mode used is Mode 1: SlfTrk. All Monte Carlo results are normalized to those by data.

5.1 Noise

The noise simulation is not ready and not applied to this study presently. Therefore, this difference should be seen in the results. It is shown directly in Fig. 8(c), in which, the noise ratios of all modules by MC are close to zero and lower than the values by data. The noise ratio by both MC and data being higher in the barrel than in the endcap, it is just the character of cosmic ray. The noise level will affect the hit number, cluster size and spacial resolution. So it can be seen that both the hit number and cluster size by MC are smaller than those by data. The long tail in Fig. 8(a) and (b) is due to the big air shower, and

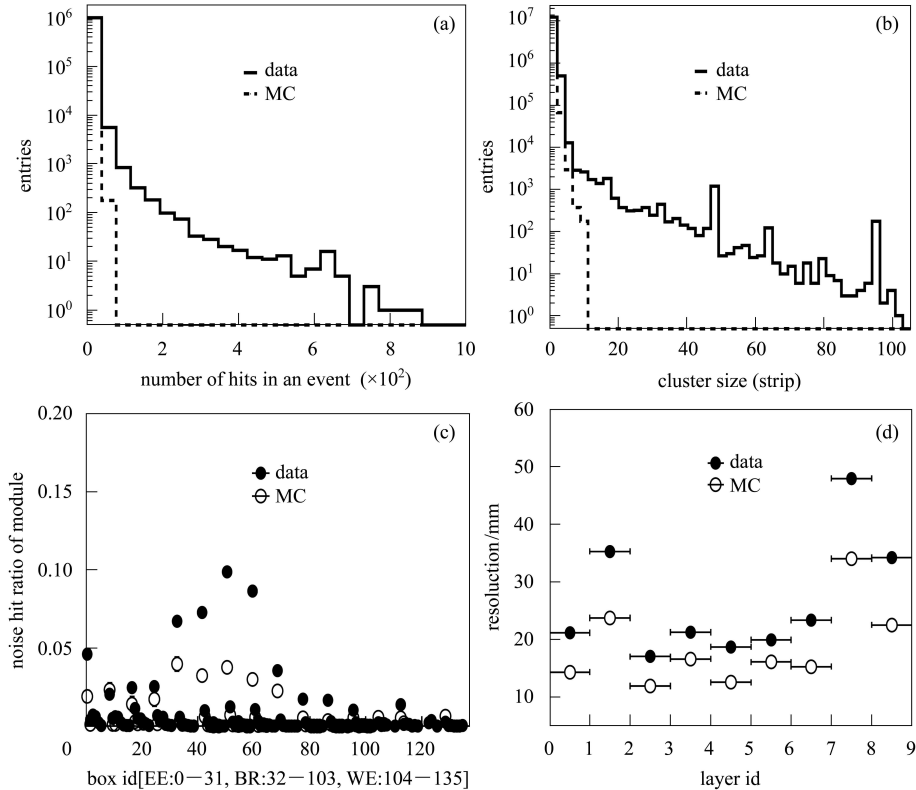


Fig. 8. The inconsistent distributions relevant to noise. (a) The number of hits in an event, (b) The cluster size distribution, (c) The noise ratio at module level, and (d) The spacial resolutions of layers in the barrel.

even possible electronics crosstalk. The resolution by MC is about 5–10 mm better than that by data at all layers. These results will be more consistent after the noise is added into the simulation and the cosmic ray generator is improved in the future.

5.2 Distribution

The comparison also can be made from some basic distributions. As shown in Fig. 9, most bins of all six distributions are consistent between MC and data. In Fig. 9(a), the number of hits in each layer matches perfectly, so does the maximum layer through by

track in Fig. 9(d). For some bins in Fig. 9(b) and (c), the MC results are lower than the data. It can be understood as the reasonable result caused by the “clean” MC and complicated real data since the noise was not added in the MC. As for the $\cos\theta$ and ϕ distributions, the small difference mainly comes from the difference of reconstruction efficiency and is affected by the incidental angle. In addition, the drop bins in Fig. 9(c) and (f) just indicate the side effect near the dead space between segments, and the dead channel near 120 in Fig. 9(b) is due to the high voltage problem in that module.

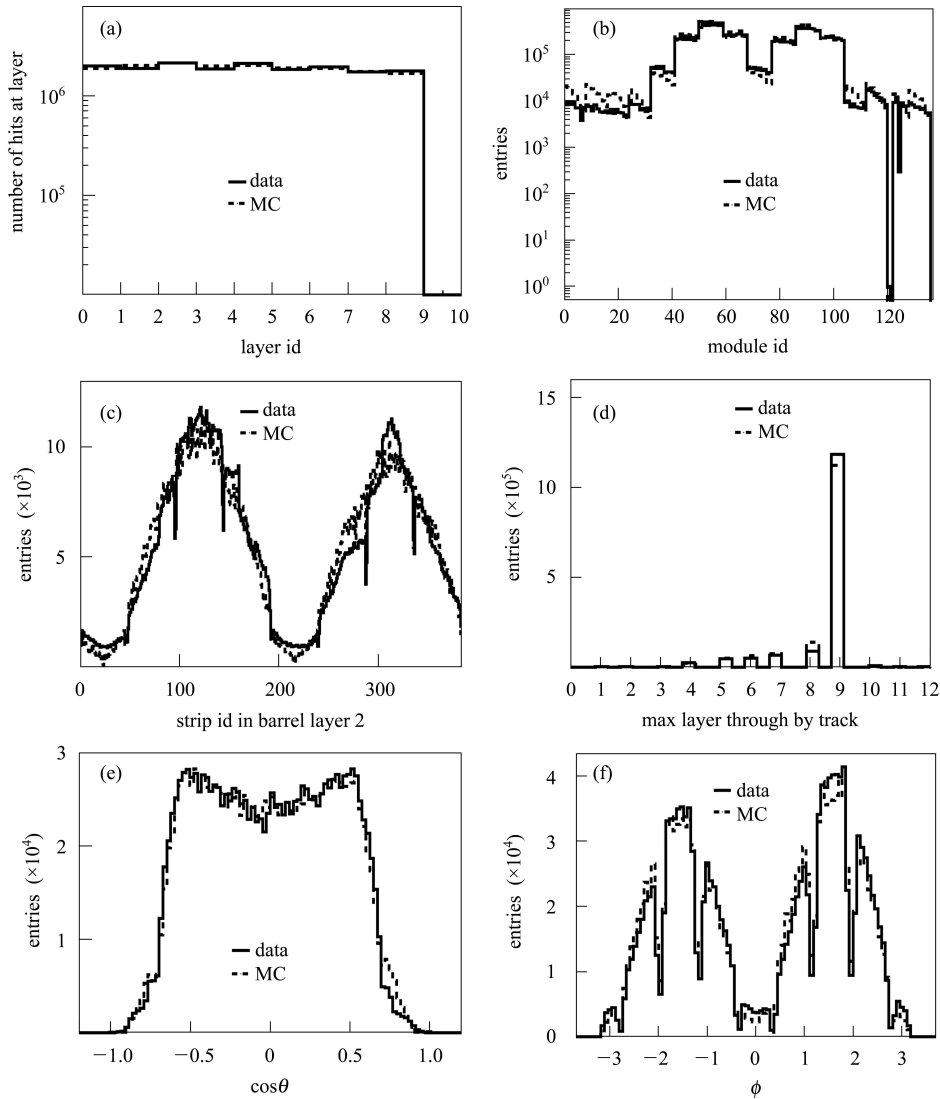


Fig. 9. The distributions comparison between MC and data. (a) The number of hits in each layer, (b) The number of hits in each module (box), (c) A hit map of layer 2 in barrel, (d) The maximum layers through by tracks. (e) and (f) are the $\cos\theta$ and ϕ of the expected position of a MUC track at the innermost layer, respectively.

5.3 Efficiency

What we are most concerned is the efficiency. In Fig. 10(a), the layer efficiency is consistent within 2%. The efficiency being lower at inner and outer two layers, to a great extent, is caused by the linear fit itself in reconstruction and few layers hit information (≤ 5) for each independent coordinate ($\Phi/Z/X/Y$). Fig. 10(c) shows the strip efficiency distributions by data and MC. Obviously, they do not match very well. For some strips, the efficiency by MC is higher than that by data, while for other strips, the result is contrary. The similar result can be seen in Fig. 10(a) and (b). The difference of strip efficiency is shown in Fig. 10(d), which gives that $\Delta\epsilon = 0.005 \pm 0.032$. So in general, the efficiency by MC is little higher than that by data, and the result is close to Fig. 6(c). The dif-

ference comes basically from, as shown in Fig. 10(e), the channels at both sides of each modules. In fact, it is very difficult to tune the MC and data matching very well at sides.

6 Summary and discussion

The calibration algorithm has been greatly improved during the BESIII commissioning. The efficiency, counting rate and noise ratio of the muon detector have been primarily calibrated by cosmic ray data, and the results are available for the simulation, reconstruction and tuning. The validity and reliability of the calibration algorithm has been checked carefully by the performance studies and comparison of Monte Carlo and data.

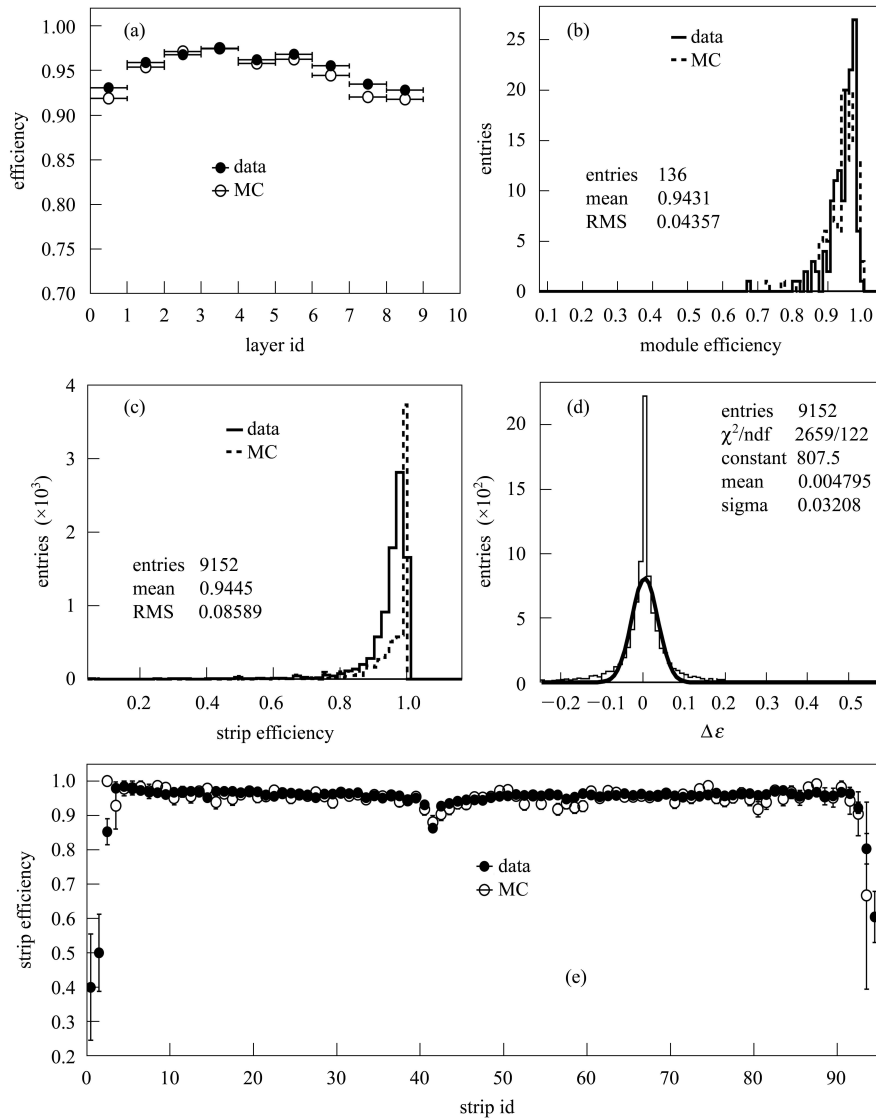


Fig. 10. The efficiency comparison between MC and data. (a) The layer efficiency, (b) The module efficiency distribution, (c) The strip efficiency distribution, (d) The efficiency difference distribution at strip level, and (e) The strip efficiency difference at Module 87 (as an example).

More detailed studies are needed and ongoing. By using dimu events, the detector alignment by software can be carried out with more precision. The effective noise simulation will make the results more consistent. The improvement of calibration also depends on the efficiency and reliability of the reconstruction.

At present, 250k events are adequate (but not enough) for a run to do the calibration. So basically, the calibration constants can be offered for each run. However, it is unnecessary to do the calibration so frequently. According to the influencing factors

in streamer mode RPC performances, the calibration must be done when one or more following situations happen: a) the high voltage or electronics threshold is changed, b) the temperature in BESIII hall changes more than 5 °C, c) the humidity in BESIII hall changes more than 20%, d) the gas mixture changes more than 1%, e) the beam status changes greatly, f) the collision energy changes, and g) the detector is repaired. All of these calibration conditions will be adjusted and determined according to the status of coming data taking.

References

- 1 WANG Yi-Fang. arXiv:hep-ex/0701010v1, 9 Jan. 2007
- 2 ZHANG Jia-Wen et al. Nucl. Instrum. Methods A, 2005, **540**: 102–112
- 3 XIE Yu-Guang et al. HEP & NP, 2007, **31**(1): 70–75 (in Chinese)
- 4 LI Wei-Dong, LIU Huai-Min et al. The Offline Software for the BESIII Experiment. Proceeding of CHEP06. Mumbai, India, 2006
- 5 LIANG Yu-Tie et al. Chin. Phys. C (HEP & NP), 2009, **33**: 666
- 6 PING Rong-Gang. Chin. Phys. C (HEP & NP), 2008, **32**(8): 599
- 7 XIE Y et al. Nucl. Instrum. Methods A, 2009, **599**: 20–27